Supplement for: Alternating Bias Assisted Annealing of Amorphous Oxide Tunnel Junctions

D. P. Pappas[1], M. Field[1],C. Kopas[1], J. A. Howard[1], X. Wang[1], E. Lachman[1], Lin Zhou[2,3], Jinsu Oh[2,3], K. Yadavalli[1], E. A. Sete[1], A. Bestwick[1], M.J. Kramer[2,3], J. Y. Mutus[1]
[1]*Rigetti Computing, 775 Heinz Avenue, Berkeley, CA 94710, USA*
[2]*Ames National Laboratory, Ames, IA 50011, USA*
[3]*Department of Materials Science and Engineering, Iowa State University, Ames, IA 50011, USA*

January 29, 2024

1 Dependence of ABAA process on junction size

Typically two different size junctions, connected in parallel, are used in order to make an asymmetric SQUID for qubit tunability. For these devices it is important that the ABAA process works for both junctions in a similar manner. This hinges on the idea that the process is voltage driven. In order to establish this, the ABAA process was conducted on similar, separate junctions. The data was taken for nominally identical parameters, i.e. voltage, pulse duration, and pulse number. Data from these studes is shown in Fig. 1(a) and (b). The statistical analysis, shown in Panel(b) demonstrating that the resistance increase, in percent, is weakly dependent on the size for this set of junctions. The mean values and uncertainties, 29 ± 1.9 for the large and 32 ± 3 for the small junctions, overlap. The Student T distributions indicate that the uncertainties are significant, hence it is important to take these differences into account when designing the SQUIDs.

2 Qubit spectroscopy and coherence

Strongly coupled TLS were studied using qubit spectroscopy of the tunable qubits across the flux period. While no strongly coupled TLS were observed in qubits treated by ABAA, in the unprocessed qubits, there were an average of 0.7 TLS/GHz seen in a 21-qubit ensemble with a 10 GHz total tunable range. Based on this, we would have expected to see ~ 3 - 4 TLS in the 9-qubit, 5.4 GHz tunable range of ABAA trimmed junctions. An example of a strongly-coupled TLS in an untreated qubit is shown in Fig 2, with the avoided level fitting shown in Fig. 3.

In addition, we show a zoomed-in version of Fig.4(a) from the paper in Fig.4. While there are small features in the spectroscopy observed in this ABAA qubit, careful analysis shows that they are due to couplings with other qubits on the chip. The salient characteristic of these features is that there is no distinct splitting observed, as shown above, that would tie these to strongly coupled TLSs in the junction.

The frequency of one ABAA-treated qubits was measured over an extended time to evaluate the stability. The mean qubit frequency over the full duration of measurements, three days in total, is 4,280.56 $\pm$ 0.001 MHz. For the subset of the data shown in Fig. 5, two protocols were used. The first protocol, i.e. "slow" measurements, averaged the Ramsey oscillation frequency for 15 minute intervals, while the "fast" measurements used a much shorter, 15 second averaging interval. This was done in order to check if there were fast jumps that were not being resolved in the slow measurements. The standard deviation over the slow measurement dataset is 0.028 MHz, and it scaled as expected for the fast measurements. No fast jumps in the frequency were observed.

Tabulations of the ABAA-treated qubit coherence values, from the data (Fig.[5] from the main paper), is shown in Table 1.

Qubit Coherence	T_1 (μs)	T_2^* (μs)	T_ϕ (μs)
ABAA treated	28.4 ± 8.7	34.1 ± 10.6	62.5 ± 23.1
80 °C annealed	20.9 ± 4.6	29.0 ± 12.7	37.9 ± 39.9
Unprocessed	19.5 ± 5.0	22.7 ± 12.3	41.4 ± 45.1

Table 1: Qubit coherence for ABAA treated, 80 ° C annealed and unprocessed qubits. The error bars are 1σ standard deviations.

3 Extracting junction critical currents

Critical currents were extracted using the transmon relations from Koch, et al.[1]. Specifically, the anharmonicity, $\alpha = \omega_{01} - \omega 12 \approx E_C$, and frequency, $\omega_{01} \approx \sqrt{8E_cE_J}$, relationships were used to find $I_0 = 2\pi E_J/\Phi_0$. The results of this are shown in Fig. 6

4 TEM characterization

Secondary electron images for the Josephson junction surface were acquired using a scanning electron microscope (SEM) (Helios, Thermo Fisher Scientific Ltd.) at 2 kV. Transmission electron microscope (TEM) samples were prepared by a focused ion beam instrument with a gas injection system (Helios, Thermo Fisher Scientific Ltd.). The TEM samples were thinned to electron beam transparency by a Ga^+ ion beam from 30 to 2 kV. The TEM samples were investigated by an aberration-corrected TEM (Titan Cube, Thermo Fisher Scientific Ltd.) at 200 kV. A high-angle annular dark-field (HAADF) detector was used for dark-field imaging in scanning TEM (STEM) mode with a convergent semi-angle and a collection semi-angle of 18 mrad and 74-200 mrad, respectively. Energy-dispersive X-ray spectroscopy (EDS) and electron energy-loss spectroscopy (EELS) studies were carried out with probe currents of 250 nA and 50 nA, respectively. Dual EELS was performed to acquire all-electron energy-loss (ELL) spectra. The plural scattering effect of all the raw ELL spectra was removed via Fourier-ratio deconvolution.

The EELS data were taken from a typical thin spot of the barrier. We do not have EELS data from the areas around grain boundary regions, but from earlier work, we observe that the oxides are significantly thicker in those regions, and hence are not expected to to participate in the tunneling process.

References

[1] J. Koch, M. Terri, J. Gambetta, A. Houck, D. Schuster, J. Majer, A. Blais, M. Devoret, S. Girvin, and R. Schoelkopf, "Charge-insensitive qubit design derived from the cooper pair box", Phys. Rev. A **76**, 042319 (2007).

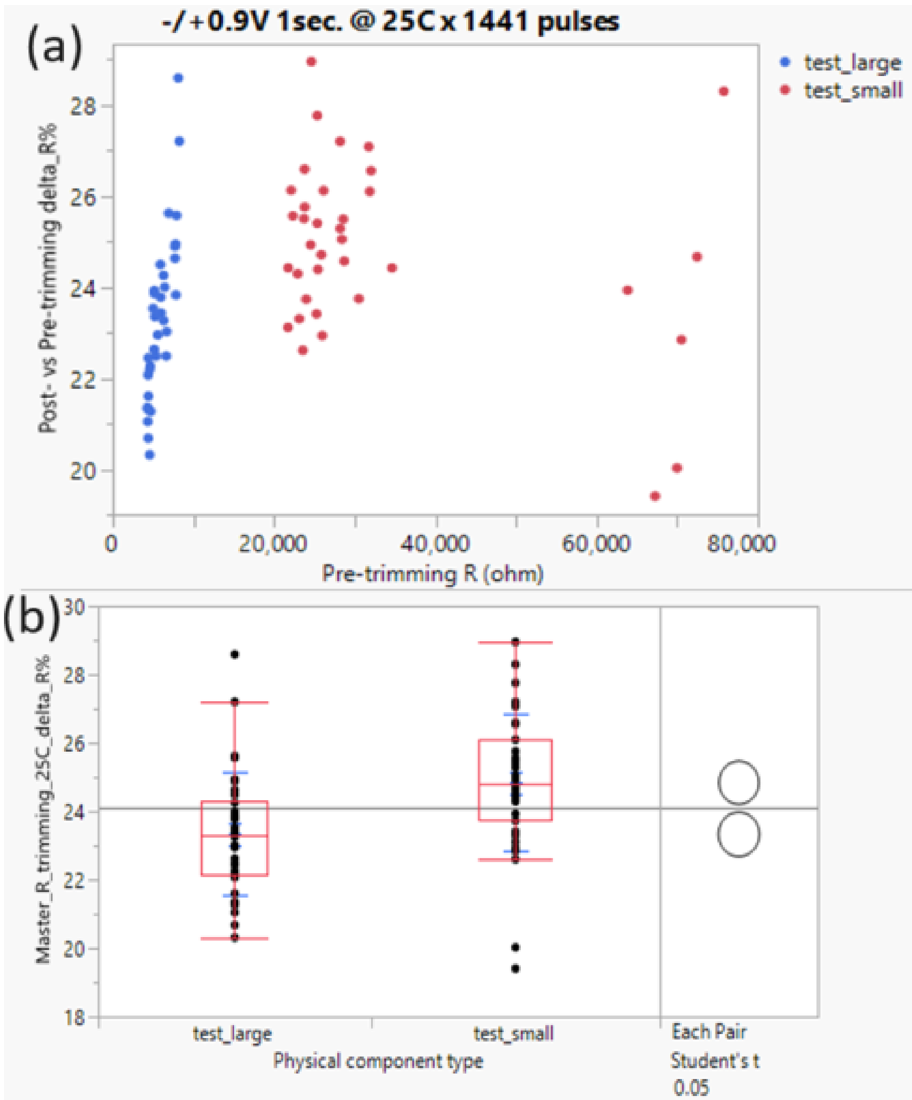

Figure 1: Dependence of ABAA trimming effect on junction resistance: Panel (a) Raw data showing resistance post-ABAA compared to resistance before. All data taken at 25 degrees; Panel (b) Date from panel (a) binned by size of junction with statistical analysis.

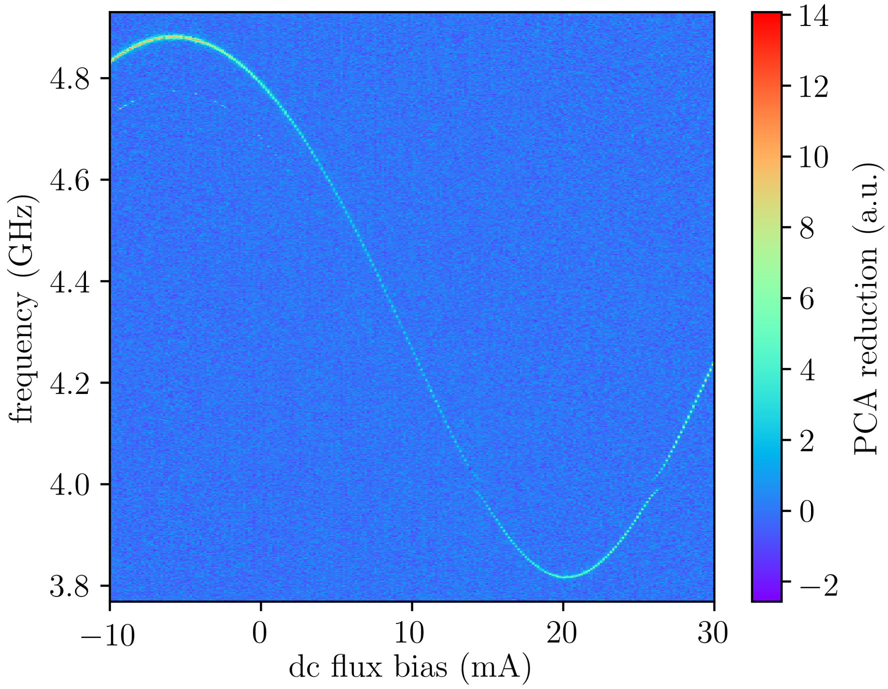

Figure 2: Untreated qubit spectroscopy illustrating a strongly coupled TLS near 4 GHz.

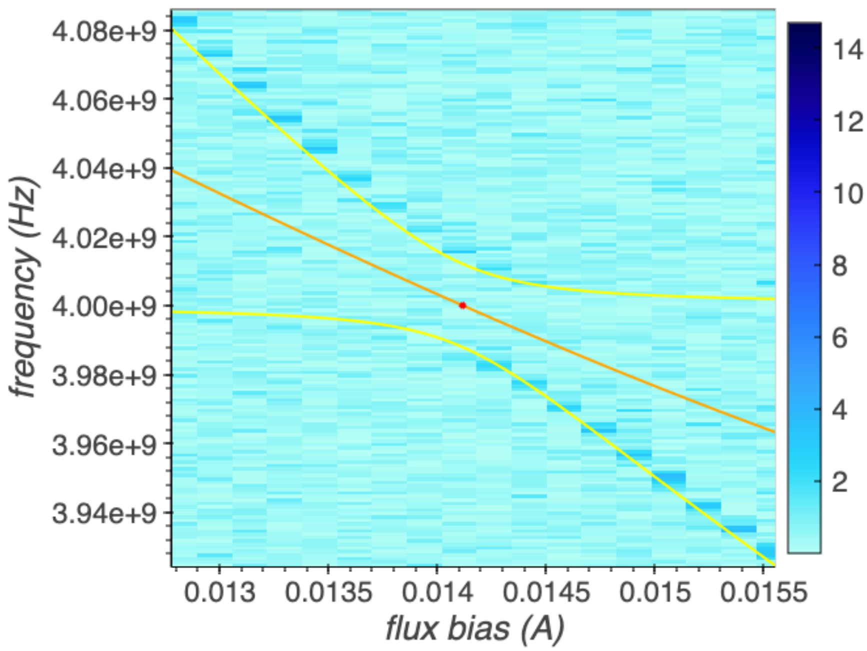

Figure 3: Fit to avoided level crossing for TLS in untreated qubit Fig. 2

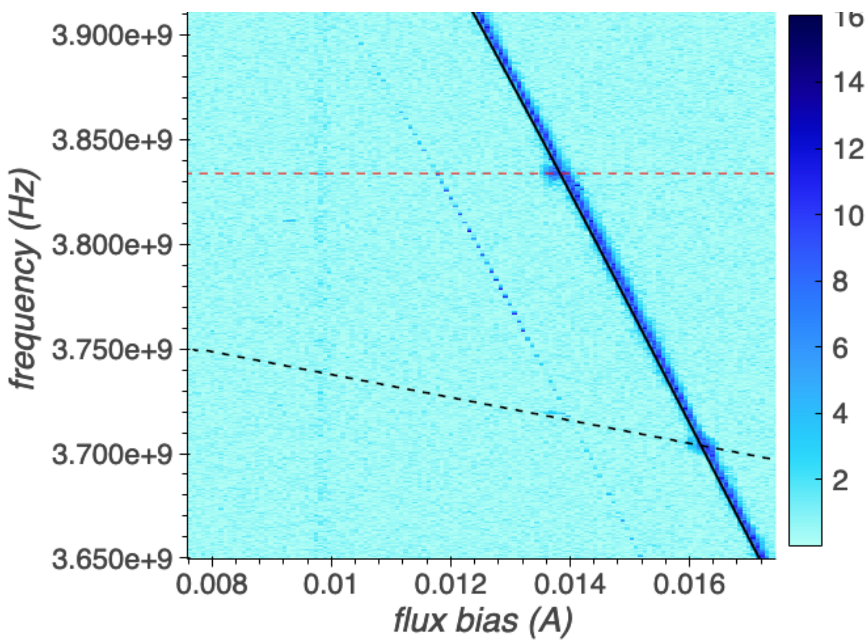

Figure 4: Zoomed in region of data from an ABAA-tuned qubit showing faint features. The red dashed line is a nearest neighbor that is a fixed qubit, and the black dashed line is a nearby tunable qubit. The $f_{02}/2$ trace is visible $\tilde{0}.11$ GHz below the f_{01}. line

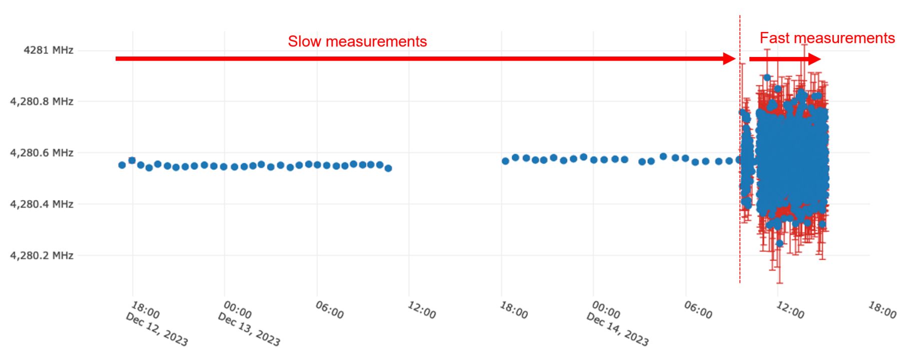

Figure 5: Time trace of a single frequency over an interval of about 46 hours.

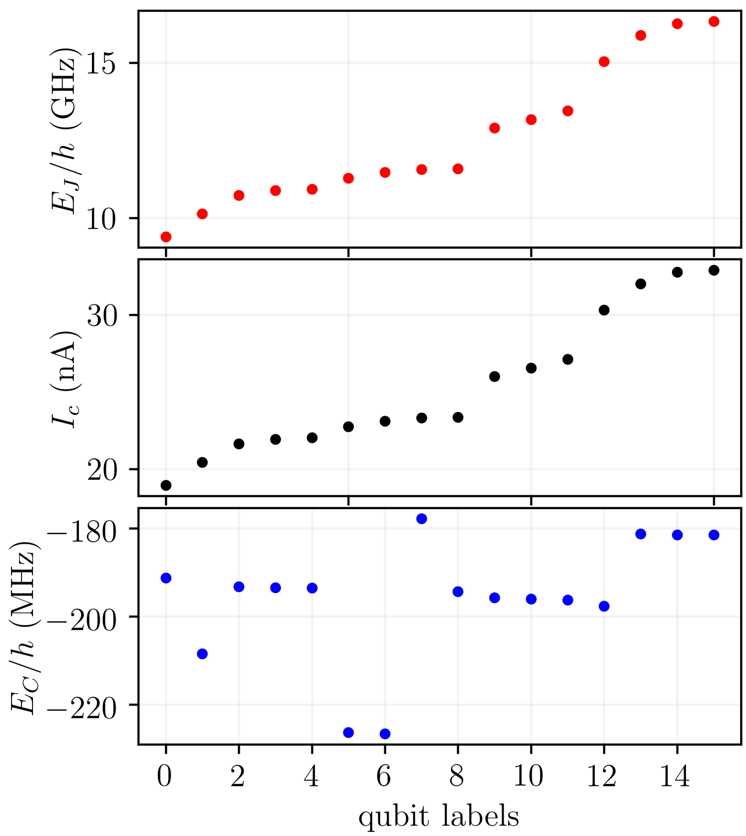

Figure 6: Top, center, and bottom panel show the values of $E_J, I_0, and E_C$ extracted from the data taken from the 15 ABAA-treated qubits.